Electroless Coating of Fe_3Si on Steels in the Molten Salt

R.O. Suzuki, T. Nishibata, Y. Nagaso, K. Nakanishi, M. Ishikawa,
K. Teranuma and K. Ono

Department of Energy Science and Technology,
Kyoto Univ., Kyoto, 606-8501 Japan

Abstract

The corrosion-resistive intermetallic compound Fe_3Si was non-electrolytically coated pure iron and mild steels. The homogenous Fe_3Si layer successfully deposited by the disproportional reaction between Si and Si^{4+} ions, using solid silicon and the molten salt composed of NaCl-KCl-NaF-Na_2SiF_6-SiO_2. The layer of Fe_3Si single phase with 24±1 mol%Si grew thicker than 200μm by immersing for a few hours at 973-1173K. The SiO_2 addition stabilized the homogeneous and repeating coating in air.

The marker experiments showed that the salt was caught up on the initial surface and left as the large voids in the layer. The Si penetration from the Fe_3Si layer into the α-Fe substrate was small due to the slow diffusion of Si in α-Fe. The fast Fe diffusion in the Fe_3Si layer left the Kirkendall holes. The quick growth of Fe_3Si wrapped the salt in the layer at the first stage of deposition.

1. Introduction

The resistance to corrosion and oxidation of iron alloys can be improved by adding appropriate amount of silicon, whereas the workability of the steel suffers by silicon addition because their strength and toughness decrease. Supposing that silicon could permeate only in the iron surface, the chemical property of iron and steel would be improved without any damage to mechanical property of the bulk [1,2].

It is electrochemically impossible that iron is electroplated with silicon in the aqueous solution. Since the early days, the gaseous deposition techniques and the solid-solid diffusion couples have been studied as silicon coating technique on iron [1,3-5]. However, these techniques handled at the temperature range higher than 1273K to promote mutual diffusion between iron and silicon.

It was reported that about 200μm thick silicides could be deposited below 1273 K on metal surface, simply by immersing the metal substrate into the molten salt composed of KCl-NaCl-NaF-Na_2SiF_6-Si [6-9]. This method is a kind of electroless plating that did not require any external energy, operable in air, and applicable to increase in scale [6,7]. When this method was applied to iron or steel, however, the formation of brittle compounds, FeSi and $FeSi_2$, were reported in addition to Fe_3Si which is known as the phase resistive to corrosion and oxidation [8,9]. Silicon was wasted for the higher silicide formation, and a subsequent annealing was need for the homogenization to Fe_3Si single phase.

The purpose of this paper is to develop the electroless plating specialized for the coating of Fe_3Si single phase on iron and steel, using the molten salt in air, and to clarify the mechanism of layer growth and defects formation. Here, some basic experimental evidence in laboratory scale is shown under the concept to consider the technical aspects for industrial application.

2. Experimental

The salt composition selected here is similar with the previous studies [6-9] as compared in **Table 1**. The composition of supporting salt is chosen referring the eutectic composition in the binary system of NaCl-KCl [10]. According to the ternary phase diagram of NaCl-KCl-NaF, the liquidus temperature is about 923 K [11]. About 150-200 g salt mixture and silicon powder was filled in the Al_2O_3 crucible. The salts mixture was heated and melted in air. Because Na_2SiF_6 is volatile above melting temperature, Oki and Tanikawa added it after melting the salt that had been once melted and solidified [8,9]. In this work, Na_2SiF_6 was initially mixed with NaCl, KCl, NaF and Si. After stirring the molten salt, the samples were immersed. The samples of high purity iron and the mild steel SS41 were fastened with pure iron wire to an alumina bar and immersed in the molten salt. For the addition of SiO_2, the transparent quartz tube was inserted for stirring into the molten salt after its melting and left in the salt during coating.

In order to mark the initial surface of iron substrate, a niobium wire of 250 μm in diameter was tightly winded to some samples. For the same purpose, silver was coated on the surfaces of some other iron samples, because Ag is immiscible both with Fe and Si at 1073 K. The wet chemical reaction for Ag coating, so-called silver mirror test, was applied by mixing the aqueous solution of $AgNO_3$ and NH_4OH with the aqueous solution of NaCl and D-Glucose. Some parts of Fe substrate had been masked by sealing tape in advance. For the better adhesion of about 1 μm thick silver layer, the coated samples were annealed at 1073 K for 72 ks in Ar gas atmosphere before dipping.

After dipping the samples were picked up from the molten salt and cooled rapidly in air. The adhered salt was removed in water, alcohol and acetone in that order. After drying, the samples was weighed and observed by optical microscope and scanning electron microscope (SEM) equipped with Energy Dispersive X-ray (EDX) analyzer. The phases on the sample surface were identified by X-ray diffraction (XRD) measurement.

3. Result and Discussion

3.1. Siliconizing mechanism

When NaF, Na_2SiF_6, and Si powder were added in the supporting salt of NaCl-KCl, the disproportional reaction between Si and Si^{4+} ions deposits the siliconized layer on the metallic substrates [7-9] as,

$$\text{Si (particles in the molten salt)} + 6F^- + SiF_6^{2-} \rightarrow 2SiF_6^{4-} \quad (1)$$

$$2SiF_6^{4-} + \text{Fe (substrate)} \rightarrow \text{Fe-Si (siliconized layer)} + 6F^- + SiF_6^{2-} \quad (2)$$

By reacting with silicon powder existing in the molten salt and Si^{4+} ion, divalent ion Si^{2+} forms as in eq.(1). Successively this Si^{2+} disproportionates on the metal surface into zero-valent Si and four-valent Si^{4+}, and the formed Si penetrates into the metal surface as in eq.(2). The total reaction,

$$\text{Si (particle in the molten salt)} + \text{Fe (substrate)} \rightarrow \text{Fe-Si (siliconized layer)}, \quad (3)$$

shows that the molten salt gives the reaction sites, and that the thermodynamic activity difference between pure silicon in the molten salt and silicon in the siliconized layer drives the reaction.

Other two possible reactions for siliconizing were discussed [7-9], where the both mechanisms can be written in the same equation, eq.(3). One is the collision that the silicon powder floating in the molten salt happens to contact with the iron surface, adheres to it, and diffuses into iron. The another is the ion exchange reaction (cementation reaction) that iron dissolves as a cation in the molten salt, and that silicon ion deposits due to the difference of electrochemical potential. The latter reaction, however, can not be deduced by extrapolating from the electrochemical properties at room temperature. Furthermore, Gay and Quakernaat [7] checked the possibility that the oxidized metal could dissolve, but they could not find any iron ion in the molten salt. Oki and Tanikawa [8,9] varied the molar ratio of Si powder, NaF and Na_2SiF_6, and they concluded that the disproportional reaction shown in eq.(1) and (2) was the main mechanism in these possibilities mentioned above.

Prior to this work, the coating mechanism was again checked. The pure Fe samples were immersed in the molten salt at 1173 K for 3.6 ks. As the extreme cases, Si powder only, Na_2SiF_6 only, or both Si powder and Na_2SiF_6, were added to the supporting salt of NaCl-KCl-NaF, as listed in **Table 2**. The mass gain per unit area of the substrate after dipping, ΔM, was small when only Si powder was added (case (a)). The previous study also reported that a very thin siliconized layer of 3-5μm was obtained at 1273 K for 18 ks, when 50mass%Si-25mass%NaCl-25mass%KCl was used [3] considering that a large amount of Si should enhance the collision.

When only Na_2SiF_6 was added (case(b)), the mass loss was recorded and no deposition was found on the surface. The surface observation and XRD showed that some portions were oxidized to Fe_2O_3, and that this iron oxide film was scratched off probably during cooling and rinsing. About 120μm thick layer was obtained in case (c) that both Si and Na_2SiF_6 were added. Therefore, neither collision mechanism nor the ion exchange could explain the larger

mass gain in case (c). These experiments support the disproportional mechanism reported [8,9].

3.2. Thickness of siliconized layer

Fig. 1 shows the mass gain per unit surface area and the thickness of the siliconized layer when the specimens of pure iron (<0.08mass%C) were immersed in the molten salt at 1173 K. As increase of immersing time, the thickness and the mass gain increased. The mass gain has a fairly good linear proportionality with the thickness of siliconized layer, although some scatters in thickness were found by observing the cross-section, as mentioned below.

Fig. 2 shows the mass gain and the layer thickness when the specimens of pure iron were immersed for 3.6 ks. As temperature increases, the thickness and the mass gain increased. They were about twice larger than those reported for pure nickel when compared at the same temperature and the same time [7].

A slight difference was detected at 1073 K between the pure iron of <0.08mass%C and the mild steel SS41 (0.16mass%C), as shown in **Fig. 3**. The results in this work were inconsistent of the previous report for the steel with low carbon content (0.1mass%C) [8,9], as shown in Fig. 3 and **Fig. 4**.

3.3. Repeated siliconizing in the same salt

The mass gain was studied when the same salt was repeatedly used. The first specimen of pure iron was immersed at 1073 K and picked up after 3.6 ks. The next new sample was successively immersed for 3.6 ks in the same molten salt. As the dipping was repeated, the mass gain for every 3.6 ks decreased as shown in **Fig. 5**. For example, the mass gain in the 6th run was 62% that of the first run. This result shows that the siliconization capacity of the repeated molten salt decreased comparing with that in the fresh salt.

Pure Na_2SiF_6 significantly evaporates above its melting point, 1120 K, by decomposing into NaF and SiF_4 gas. The vapor pressure of SiF_4 in equilibrium with pure Na_2SiF_6 thermodynamically exceeds the atmospheric pressure above 866 K [12]. The addition of LiF was reported to stabilize significantly SiF_6^{2-} ions in the salt, but the Si content reduced to about a half for a few hours at 723 K [13]. Although NaF instead of LiF was added for stabilization of the SiF_6^{2-} ions in this work, and the metallic silicon continuously supplied Si ions by the disproportional reaction, we worried that the silicon loss by evaporation could not be neglected at the elevated temperatures. Unfortunately the chemical analysis of Si content in the molten salt used did not show the reproducible values. Supposing that the dissolving speed from metallic silicon is slow, i.e., fresh supply of Si ions is delayed, the amount of siliconized layer can be decreased because of SiF_4 evaporation during long dipping time. Therefore, it may be important to maintain Si ion content high enough to siliconize the substrate.

3.4. SiO_2 addition

Inserting the SiO_2 tube into the molten salt, the dipping was repeated as mentioned above. It was clear that a certain amount of SiO_2 dissolved, judging from the fact that the thickness of the transparent quartz tube (1 mm) was halved after the experiments. By adding SiO_2, the time dependency of mass gain per 3.6 ks was suppressed as shown in Fig. 5, and the similar thickness was obtained at 1073 K at least to 28.8 ks. This stabilization of siliconizing is because the silicon ion concentration in the molten salt maintained nearly constant, balancing silicon loss both for siliconizing and evaporation against silicon supply both from Si and SiO_2.

Fig. 6 shows the mass gain per unit area of the pure iron samples when SiO_2 was thus supplied. All the data in Fig. 6 were obtained using the fresh salt. The effect of SiO_2 existence

on mass gain was small as compared with the data in Fig. 1, 3 and 4. This shows that the chemical activity of Si^{2+} ions existing in the molten salt was enough for siliconizing whether SiO_2 exists or not, and that the layer growth probably depends on the diffusion in the layer. By adding SiO_2, however, the homogeneity of layer thickness in a specimen was improved, comparing with the data for no addition. This may present that the concentration of Si^{2+} ions was homogenized in the molten salt by inserting SiO_2 tube.

When the molten salt containing of metallic silicon is used in air, a part of Si may be oxidized to SiO_2 by atmospheric air and it supplies Si^{2+} ions to the salt. This merit was not stated in the previous works [7-9], although they melted the salt in open air.

3.5. Structure of siliconized layer

Fig. 7 shows the siliconized surface of the pure iron specimens immersed with SiO_2 tube. The equiaxed grains with the similar size covered the substrate smoothly. The coarser grain size was obtained as the higher temperature and as the longer immersing time.

The XRD measurements identified that all these grains were single phase of Fe_3Si with DO_3 crystal structure, whether SiO_2 coexisted or not, and whether the substrate was pure iron or mild steel SS41. Oki and Tanikawa [8,9] reported that Fe_3Si was formed near Fe substrate, but that both FeSi and $FeSi_2$ were also formed near the layer surface. They identified the dominant phase in the layer as FeSi. It is not consistent with this work. This difference of formed phases reflects the discrepancy in the amount of siliconizing, as shown in Fig. 3 and 4. The details will be discussed later.

3.6. Profile of Si concentration

Fig. 8 and **Fig. 9** show the cross-sectional SEM images of these samples. The white lines in these figures show the X-ray intensity of Si-Kα, i.e., Si concentration along the cross-section. For all the samples of pure Fe and SS41, the silicon profiles were almost flat inside the siliconized layer and commonly dropped to zero at the interface. No silicon was detected at the α-Fe substrate inside the layer. The quantitative analysis by EDX showed that Si concentration in the layer was constantly 24±1mol%Si, although Fe_3Si has a wide range of stoichiometry, i.e., 10-25at%, according to the accepted phase diagram [14]. The concentration higher than the stoichiometric Fe_3Si was incidentally detected at the top surface, and it was not known whether it was the silicon fine powder adhered to the surface, thin oxidized film such as SiO_2, or the higher iron silicide such as FeSi. Judging from XRD analysis, the volume fraction of these possible phases should be less than 1%. Neither Si concentration gradient[3] nor the graphite precipitation[8,9] was detected in the layer.

3.7. Markers of initial surface

As shown in **Fig. 10**, the thin Fe_3Si layer was also formed under the Nb marker, although the Nb wire was winded up tightly to the initial surface. The curved interface indicated that there might have been some space where the molten salt could penetrate, or that a small amount of silicon diffused round the marker. The Nb marker experiment showed that the initial surface located at least in the Fe_3Si layer, not at A in Fig. 10.

As shown in **Fig. 11**, the masked Ag layer remained after dipping at 1073 K for 7.2 ks. When the flat surfaces at the masked area are interpolated, the location of the initial Fe surface can be clearly imagined. The Ag layer at the central part of Fig. 11 was eroded and pushed toward the interface, judged by connecting the isolated Ag particles. The white particles of Ag located with the holes near the interface, and all the voids exist over these Ag particles. This means that the voids might be introduced at the earlier stage of the Fe_3Si formation. Many small holes were found in the Fe_3Si layer near the interface, namely, at the

position between the iron substrate and its initial surface.

The inclusions in the siliconized layer, as observed commonly in the cross-sectional views, were the metallic Si grains. Because the Si powder used was suspended in the molten salt, it was caught into the layer. The Si powder located above the voids and it was wrapped in the Fe_3Si layer, as shown in Fig. 11.

3.8. Impurities in the voids

By bending the siliconized plates, the Fe_3Si layers pealed off from the substrates. The fracture was occurred along the voids in the Fe_3Si layer, but more often along the interface. A cross-section of the fractured layer was observed as shown in **Fig. 12**, where the right side of the film was detached from the substrate. The distribution of the salt components was analyzed as in Fig. 12. Because the molten salt attached on the specimen was not removed artificially, the some components of the salt, Si, Na, K, and Cl, were detected from the left side of this film. It is interesting that these elements were also detected from another side. Because the components of the molten salt are easily soluble in the aqueous solution, it was not easy to find their existence in the cross-section after mechanical polishing using water. The salt components in the layer always existed only in the voids and near Si particles, not in the small holes. Most of the voids usually contained the salt.

The reason of salt enclosure will be clarified by knowing when the voids were formed. The position of voids as shown in Fig. 11 indicates that the voids might be formed at the earlier stage of layer formation. The samples dipped in the molten salt for the time shorter than 0.3 ks, however, did not form the homogenous and smooth layer. Almost parts of the layer were cracked and separated from the substrate. The void formation and the salt trap could not be specified in these samples.

Another possibility of the existence of salt components in the layer is that the molten salt invaded into the open voids through the micro-cracks, which might be produced in cooling by the difference of thermal expansion coefficients of Fe_3Si and Fe. Judging from marking experiments by adding AgCl into the molten salt, this assumption was not realistic; the molten salt left in the Fe_3Si layer was enclosed not at the final stage such as in quenching, but at the initial stage of siliconizing.

4. Discussion

4.1. Formation of Fe_3Si by diffusion

The diffusion constants reported were summarized in **Fig. 13** [15]: The Si diffusion in α-Fe phase (A2 structure) is about a few times faster than Fe diffusion. Fe diffusion is significantly enhanced in Fe_3Si phase, and depressed in the FeSi. It is noted that Si diffusion in Fe_3Si phase is much slower than that in α-Fe phase.

These diffusion data in the Fe-Si system may clarify the layer formation reported by Ivey *et al*. [1,17]: They contacted pure Si and pure Fe, and found that $FeSi_2$, FeSi and Fe_3Si were formed between two pure elements as imagined from the phase diagram. They reported that Fe_3Si was formed preferentially and the other silicides were formed later. Considering the diffusivity summarized in **Fig. 13**, we can understand that the slow Si supply through FeSi layer and the fast Fe diffusion through Fe_3Si phase could form the Fe_3Si layer as the dominant phase.

The other intermetallic compounds such as $FeSi_2$ or FeSi could be thermodynamically

formed also in the present work, because the chemical activity of silicon was kept high in our molten salt. Supposing that the precipitation of silicon from the molten salt was slow, namely, the Si transfer from the molten salt to the siliconized layer was as slow as that in the diffusion couple, the fast Fe diffusion through Fe_3Si phase may not allow forming the higher silicides. Once these compounds were formed, they would be diluted by Fe and transformed into Fe_3Si.

4.2. A model for Fe_3Si layer growth

Fast layer formation of Fe_3Si is noteworthy for the industrial application. About 120μm thick layer could be deposited within 1 hour at 1173 K. Here we will construct a model to express the growth of Fe_3Si layer from the diffusivity of Fe and Si. **Fig. 14** illustrates a model based on the experimental data for pure Fe substrate.

(1) Reaction Front

The deposited silicon by the disproportional reaction initiates the Fe_3Si grains on the iron surface (**Fig. 14(1)**). For the growth of the individual Fe_3Si grain, the mutual diffusion between Fe and Si need occur. Since Fe can diffuse much faster than Si in Fe_3Si grain, Fe atoms are quickly supplied to the Fe_3Si surface through Fe_3Si, where they wait for Si arrival and react with Si. Thus the new formation of Fe_3Si is considered to occur preferentially at the Fe_3Si surface.

(2) Salt Trapping

The preferential directional growth of Fe_3Si grains may occur, for example, keeping a crystallographic orientation of the substrate. Although the epitaxy with the substrate was not studied, it should be noted that the DO_3 structure of Fe_3Si is the ordered phase of A2 structure. These grains surround the molten salt near the initial surface, and a part of the salt is captured in the Fe_3Si layer. Because of coexistence with the molten salt, the adhesion of the Fe_3Si grains on the surface becomes weak as the whole layer. This initial stage of Fe_3Si growth (**Fig. 14(2)**) might be hardly observed, even if the sample could be quenched after a short dipping time.

(3) Kirkendall Holes

As indicated in Fig. 10 and 11, iron diffused out to the surface, and the initial surface was pulled inside the substrate. Once Fe_3Si covers the whole initial surface of pure Fe substrate (**Fig. 14(3)**), the total Fe supply to the reaction front is enhanced through the tight Fe_3Si layer. With movement of the initial surface into the iron bulk, the Kirkendall holes also shift into the bulk and some holes is crushed into the elliptical shape. In the worst case, these holes connect each other and make a crack at the interface between the Fe_3Si layer and the substrate (**Fig. 14(4)**).

(4) Si Trapping

Because the Si particles suspend in the molten salt, they may be surrounded in the Fe_3Si layer (**Fig. 14(4)**), when they happen to attach on the sample surface. These Si particles captured in the layer, however, hardly reacted with the Fe_3Si layer to form the higher silicides, and hardly enhanced the Fe_3Si formation. The former phenomenon reflects the evidence that the higher silicide formation was delayed when pure Si and Fe were contacted [N20,N21]. The latter suggests that the reactivity when silicon was supplied continuously from the molten

salt is higher than that when solid silicon was attached.

(5) Cracks in the layer

Oki and Tanikawa [8,9] developed the silicide coating using the same molten salt as this work. They identified the dominant phase in the layer as FeSi, not Fe_3Si. It can be understood as the difference of siliconizing ability due to Si^{2+} ion concentration in the molten salts. However, the crack formation at the interface may give another reason of the discrepancy in phase formation. Once the crack initiate at the interface, Fe supply to the surface become insufficient for Fe_3Si formation, and the higher silicides can be formed at the Si side. This phenomenon due to crack initiation was detected in the Fe/Si diffusion couple [16,17].

Although the siliconized iron itself was corrosion resistive [8,9], the coexistence of salt in the Fe_3Si layer is not favorable. Because the Fe_3Si is electrochemically nobler than Fe, the cracks significantly weaken the corrosion resistance. The remained salt may enhance the corrosion once a crack arrives to it.

The Si addition to the bulk could signicifantly decrease the voids related with the molten salt [15]. The addition over 15% can completely remove the Kirkendall holes, although the mechanical properties of bulk materials are scarified. Further progress can be expected by controlling the growth rate.

Conclusion

Using silicon deposition from the molten salt, which is mainly caused by the disproportional reaction, the intermetallic compound, Fe_3Si, was smoothly coated in air both on the pure iron and the low carbon steel, SS41. The coated layer was the single phase of DO_3 crystal structure with about 24±1 mol%Si. This siliconizing method depends on the continuous reaction between solid silicon and Si^{4+} ion in the salt composed of KCl-NaCl-NaF-Na_2SiF_6-Si. When the Si^{4+} ion source was only Na_2SiF_6, the siliconizing rate decreased because of SiF_4 evaporation. When SiO_2 was added to the molten salt, the siliconizing became stable. Because the high content of Si ion could be hold in the molten salt, the Fe_3Si layer grew thicker than 200μm for a few hours at 1173K. The formation of the higher silicides such as FeSi and $FeSi_2$ reported previously was not observed in the layer. It might be caused by poor Fe supply to the layer through the crack.

The marker experiments using Nb wire, and Ag coating showed that the salt was caught up on the initial surface and left as the large voids in the layer. The fast deposition of silicon on pure iron surface and the quick growth of Fe_3Si wrapped the salt in the layer at the first stage of deposition. Based on the reported diffusivity data, the slow Si penetration from the Fe_3Si layer into the α-Fe substrate is reasonable. The fast Fe diffusion in the Fe_3Si layer left the Kirkendall holes.

Acknowledgement

The authors thank Mr. T. Unesaki and Mr. I. Nakagawa for SEM-EDX analysis. This study was supported in part by Grants-in-Aid for Scientific Research, under Contract No. 10555256.

References

1. *Ihrig, H.J.:* Metal Progress, [4] (1938), p.367/372.
2. *Saldanha, B.J.; Streicher, M.A.:* Materials Performance, 25 (1986), p.25.
3. *Hosokawa, K.:* J. Jpn. Inst. Met., 39 (1975), p.345/351 (in Japanese).
4. *Hirai, S.; Ueda, S.:* Trans. Jpn. Inst. Met., 29 [8] (1988), p.685/692.
5. *Stetsovskii, L.L.; Shvartsman, L.A.:* Izv. Akad. Nauk SSSR. Metally. [3] (1991), p.180/185 (in Russian).
6. *Belyaeva, G.I.; Anfinogenov, A.I.; Ilyushchenko, N.G.:* Metalloved. I Term. Obrabotka Metal. Sb. Statei, 13 (1971), p.63/65 (in Russian).
7. *Gay, A.J.; Quakernaat, J.:* J. Less-Comm. Metals, 40 (1975) p.21/28.
8. *Oki, T.; Tanikawa, J.:* J. Metal Finishing Soc. (Kinzoku Hyohmen Gijutsu), 31 [10] (1980), p.561/566 (in Japanese).
9. *Oki, T.; Tanikawa, J.:* Molten Salt (Yoyuen), 25 [2] (1982), p.115/137 (in Japanese).
10. *Sangster, J.M.; Pelton, A.D.:* Phase Diagrams for Ceramists, Vol.VII, ed. by Cook, L.P. and McMurdie, H.F., The Amer. Ceramic Soc. Ohio, (1989) p.205/206.
11. *Sauerwald, F.; Dombois H.E.:* Z. Anorg. Allgem. Chem., 277 (1954), p.70 (in German).
12. *Kubaschewski, O.; Alcock, C.B.; Spencer. P.J.:* Materials Thermochemistry, 6th Ed., Pergamon Press, Oxford, (1993), p.296.
13. *Ueda, T.; Goto, T.; Ito, Y.:* J. Surface Finishing Soc. of Japan (Hyohmen Gijutsu), 46 [12] (1995), p.1173/1179 (in Japanese).
14. *Kubaschewsk, O.:* Iron - Binary Phase Diagrams, Springer-Verlag, New York, (1982) p.136/139.
15. *Suzuki, R.O.; Nagaso, Y.; Nakanishi, K.; Ono, K.:* steel research, accepted for publication.
16. *Baldwin, N.R.; Ivey, D.G.:* J. Phase Equil., 16 [4] (1995) p.300/307.
17. *Zhang, Y.; Ivey, D. G.:* J. Mater. Sci., 33 [12] (1998), p.3131/3135.
18. *Mirani, H.V.M.; Maaskant, P.:* Phys. Stat. Sol., (a) 14 (1972) p.521/525.
19. *Mitani, H.; Onishi M.; Kawaguchi, M.:* J. Jpn. Inst. Met., 31[12] (1967) p.1341/1344 (in Japanese).
20. *Mirani, H.V.M.; Harthoorn, R.; Zuurendonk, T.J.; Helmerhorst, S.J.; de Vries, G.:* Phys. Stat. Sol., (a) 29 (1975) p.115/127.
21. *Oviedo de Gonzalez, C.; Walsoe de Reca, N.E.:* J. Phys. Chem. Solids, 32 (1971), p.1067/1074.
22. *Million, B.:* Czech. J. Phys., B 27 (1977) p.928/934.
23. *Treheux, D.; Vincent, L.; Guiraldenq, P.:* Acta Metall., 29 (1981) p.931/938.
24. *Raghunathan, V.S.; Sharma, B.D.:* Phil. Mag. A, 43 [2] (1981) p.427/440.
25. *Borg, R.J.; Lai, D.Y.F.:* J. Appl. Phys., 41 [13] (1970) p.5193/5200.
26. *Gude, A.; Hehrer, H.:* Philos. Mag. A, 76 [1] (1997) p.1/29.
27. *Salamon, M.; Hehrer, H.:* Philos. Mag. A, 79 [9] (1999) p.2137/2155.

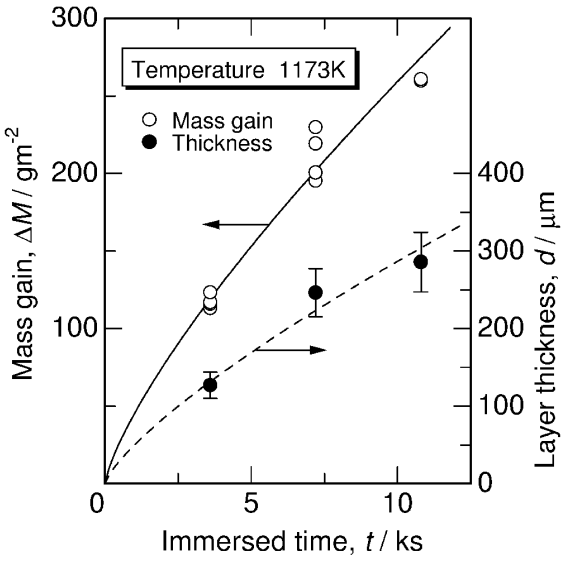

Fig. 1 Mass gain and layer thickness of the pure iron specimens siliconized at 1173 K as a function of immersed time.

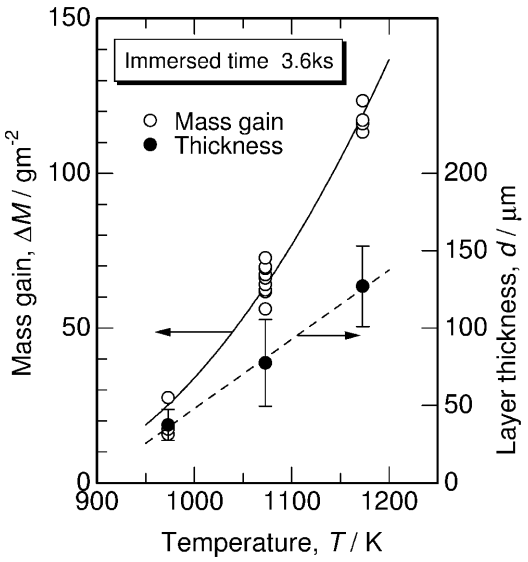

Fig. 2 Mass gain and layer thickness of the pure iron specimens siliconized for 3.6 ks as a function of immersed temperature.

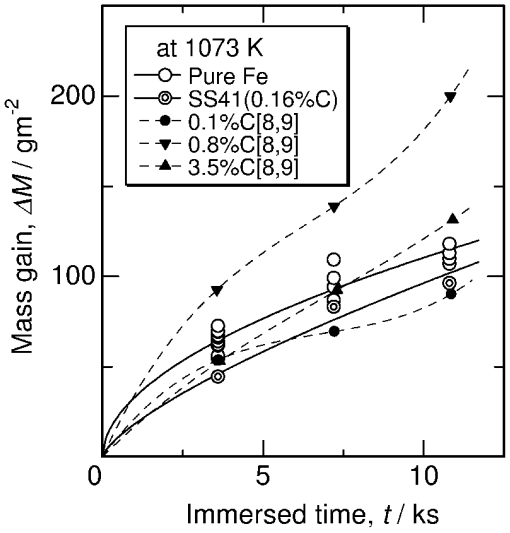

Fig. 3 Mass gain of the specimens as a function of immersed time at 1073 K.

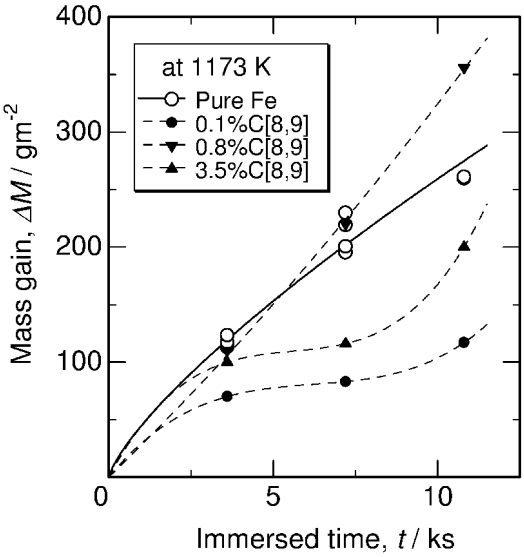

Fig. 4 Mass gain of the specimens as a function of immersed time at 1173 K.

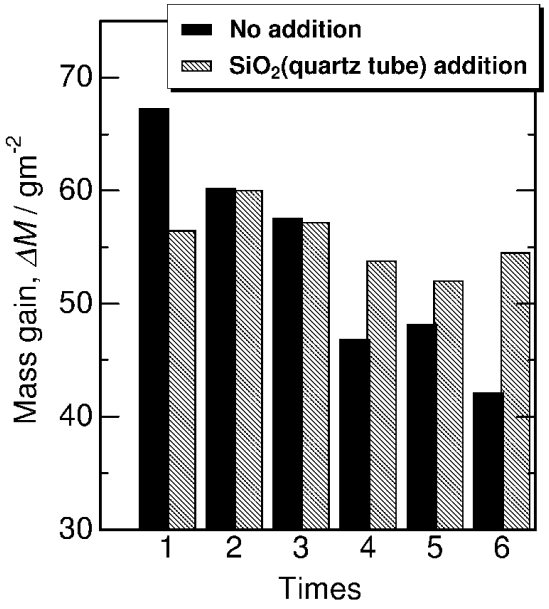

Fig. 5 Mass gain of pure iron for every 3.6 ks at 1073 K.

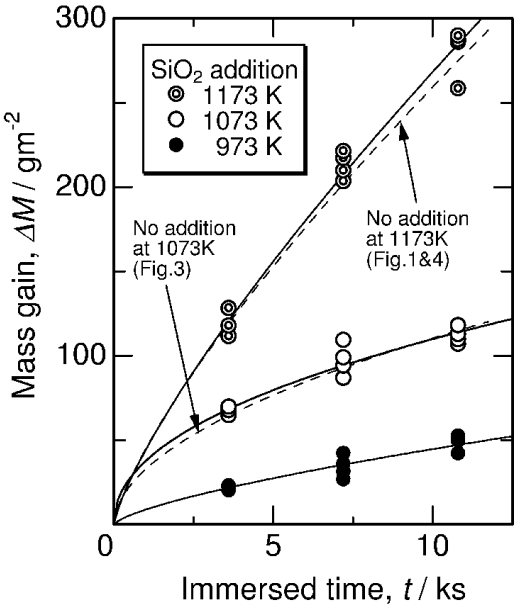

Fig. 6 Mass gain of the pure iron specimens as a function of time immersed with SiO_2 tube.

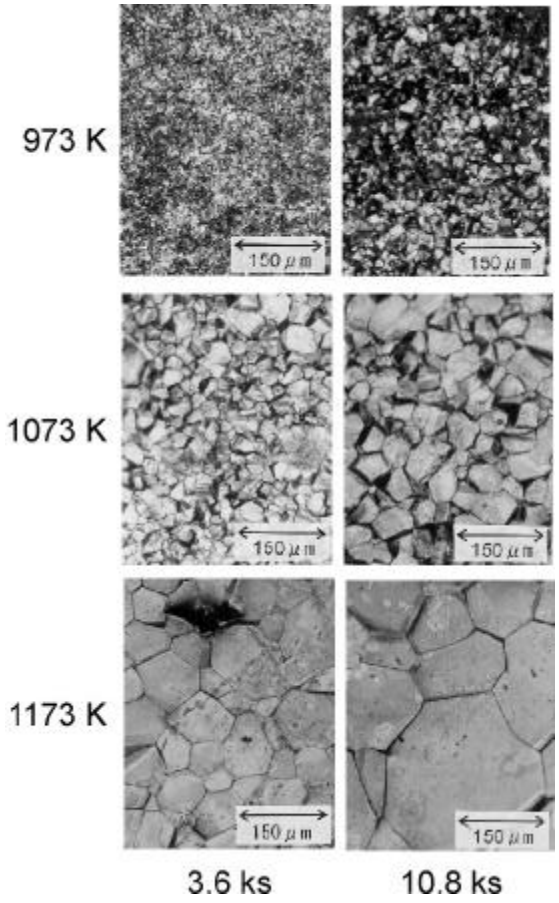

Fig. 7 Optical micrographs of the siliconized surface of pure iron specimens.

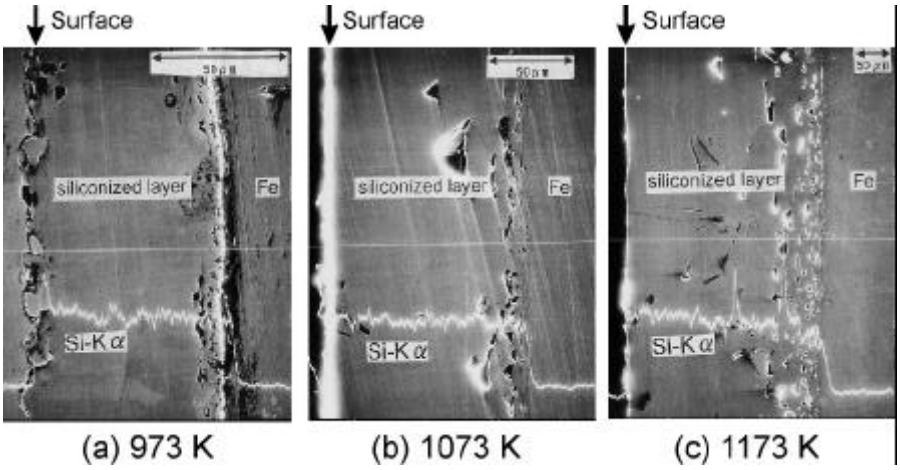

Fig. 8 Scanning electron micrographs of the cross-section for pure iron specimens siliconized for 10.8 ks. Si-Kα X-ray intensity was analyzed along the white line.

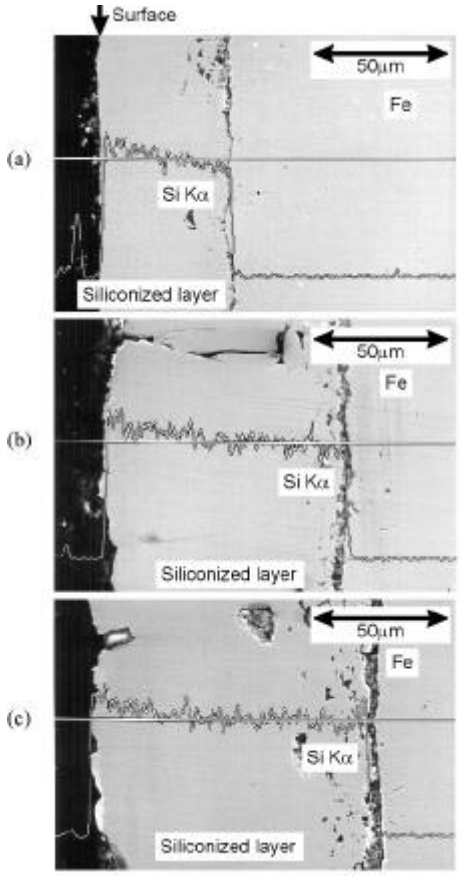

Fig. 9 Scanning electron micrographs of the cross-section for the mild steel SS41 siliconized at 1073K for 3.6 ks (a), 7.2 ks (b) and 10.8 ks(c), respectively.

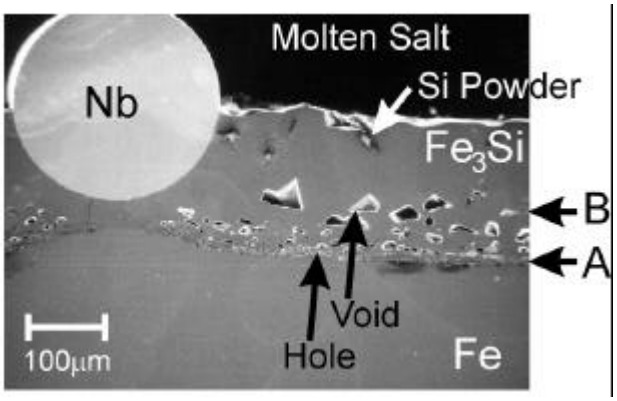

Fig. 10 Scanning electron micrograph of the cross-section for pure iron specimen siliconized at 1073 K for 18 ks.

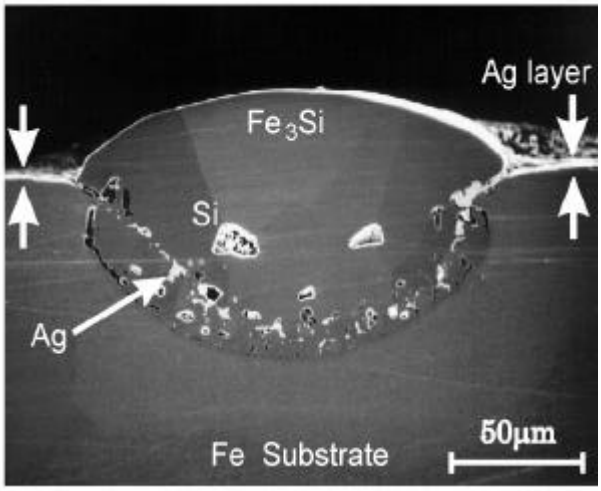

Fig. 11 SEM image of the cross-section for Fe substrate after Ag coating and subsequent siliconizing.

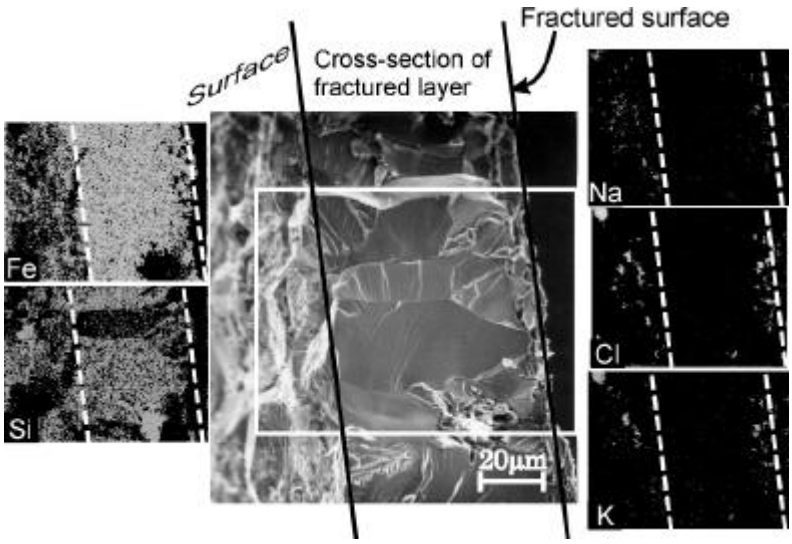

Fig. 12 Distribution of Fe, Si, Na, Cl and K at the area enclosed by white rectangle in the fractured Fe_3Si layer, where the solidified molten salt was not rinsed.

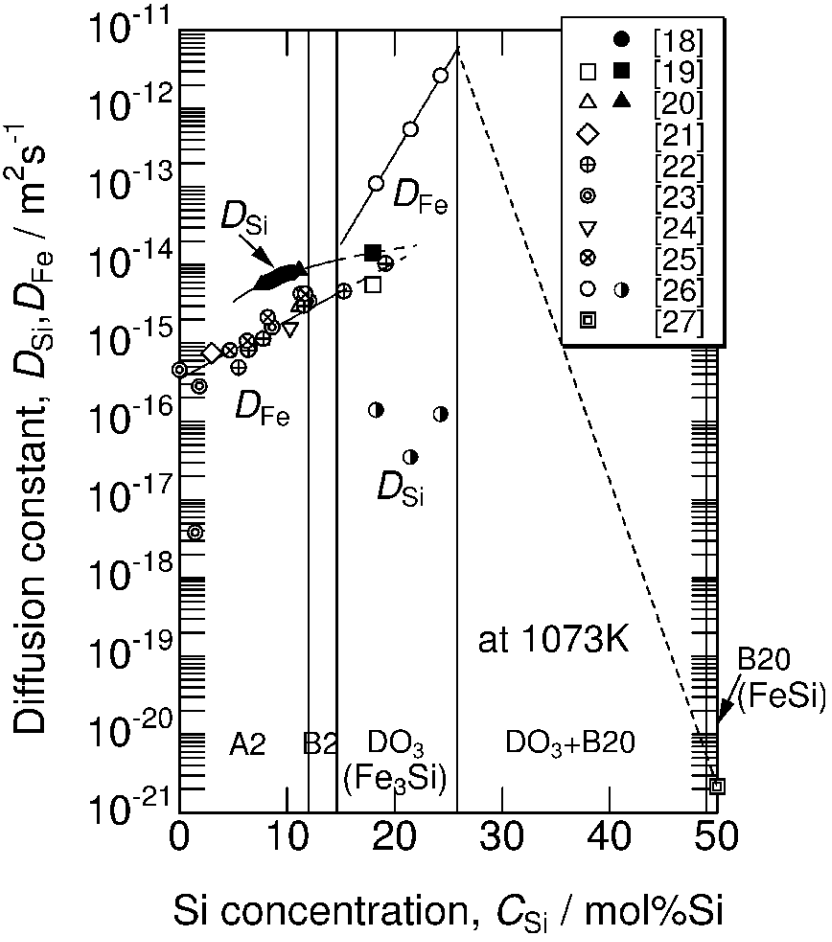

Fig. 13 Diffusion constants of Si and Fe at 1073K.

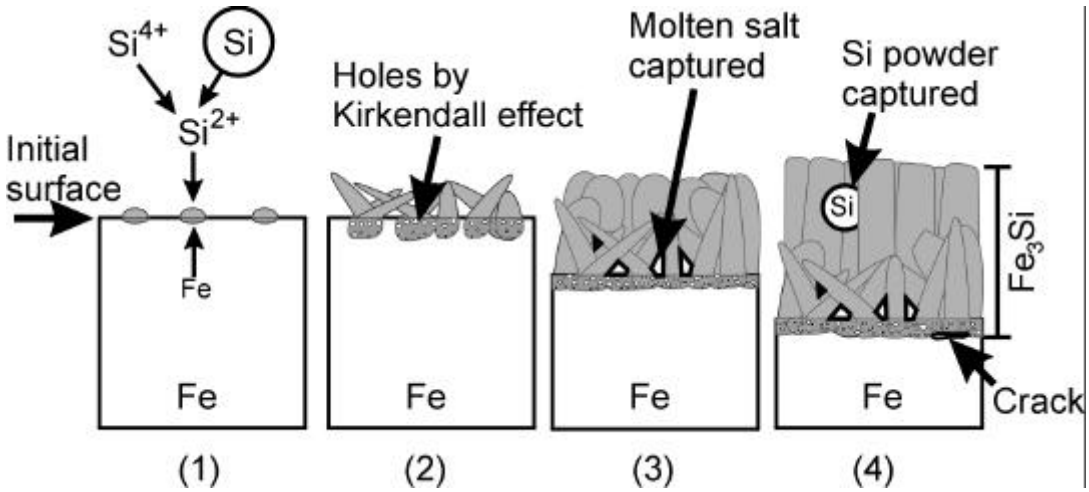

Fig. 14 A growth model of the Fe_3Si layer.

Table 1: Salt compositions and the amounts of additional metallic silicon.

	Salt composition (% in molar fraction)						
	NaCl	KCl	NaF	Na_2SiF_6	Sub total	Metallic Si	Total
Eutectic composition [10]	50.6	49.4	____	____	100	____	____
Hosokawa [3]	50	50	____	____	100	100	200
Belyaeva et al. [6]	40.88	32.05	22.13	4.94	100	23.63	123.63
Gay and Quakernaat [7]	40.88	32.05	22.13	4.94	100	23.63	123.63
Oki and Tanikawa [8,9]	40.98	32.12	22.00	4.90	100	22.05	122.05
This work	36.58	36.58	21.95	4.89	100	21.85	121.85

Table 2: Mass gain of the pure iron specimens after immersing at 1173 K for 3.6 ks in the molten salts, where the molar ratio of the components was commonly kept as NaCl : KCl : NaF = 36.58 : 36.58 : 21.95.

Run No.	Components in the molten salt bath (molar ratio)					Mass gain, ΔM (gm^{-2})
	NaCl	KCl	NaF	Na_2SiF_6	Si	
(a)	36.58	36.58	21.95	0	21.85	8
(b)	36.58	36.58	21.95	4.89	0	-100
(c)	36.58	36.58	21.95	4.89	21.85	120